
WRL

Research Report 90/9



Pool Boiling Enhancement Techniques for Water at Low Pressure

Wade R. McGillis
John S. Fitch
William R. Hamburgen
Van P. Carey

The Western Research Laboratory (WRL) is a computer systems research group that was founded by Digital Equipment Corporation in 1982. Our focus is computer science research relevant to the design and application of high performance scientific computers. We test our ideas by designing, building, and using real systems. The systems we build are research prototypes; they are not intended to become products.

There is a second research laboratory located in Palo Alto, the Systems Research Center (SRC). Other Digital research groups are located in Paris (PRL) and in Cambridge, Massachusetts (CRL).

Our research is directed towards mainstream high-performance computer systems. Our prototypes are intended to foreshadow the future computing environments used by many Digital customers. The long-term goal of WRL is to aid and accelerate the development of high-performance uni- and multi-processors. The research projects within WRL will address various aspects of high-performance computing.

We believe that significant advances in computer systems do not come from any single technological advance. Technologies, both hardware and software, do not all advance at the same pace. System design is the art of composing systems which use each level of technology in an appropriate balance. A major advance in overall system performance will require reexamination of all aspects of the system.

We do work in the design, fabrication and packaging of hardware; language processing and scaling issues in system software design; and the exploration of new applications areas that are opening up with the advent of higher performance systems. Researchers at WRL cooperate closely and move freely among the various levels of system design. This allows us to explore a wide range of tradeoffs to meet system goals.

We publish the results of our work in a variety of journals, conferences, research reports, and technical notes. This document is a research report. Research reports are normally accounts of completed research and may include material from earlier technical notes. We use technical notes for rapid distribution of technical material; usually this represents research in progress.

Research reports and technical notes may be ordered from us. You may mail your order to:

Technical Report Distribution
DEC Western Research Laboratory, UCO-4
100 Hamilton Avenue
Palo Alto, California 94301 USA

Reports and notes may also be ordered by electronic mail. Use one of the following addresses:

Digital E-net:	DECWRL : WRL-TECHREPORTS
DARPA Internet:	WRL-Techreports@decwrl.dec.com
CSnet:	WRL-Techreports@decwrl.dec.com
UUCP:	decwrl!wrl-techreports

To obtain more details on ordering by electronic mail, send a message to one of these addresses with the word "help" in the Subject line; you will receive detailed instructions.

Pool Boiling Enhancement Techniques for Water at Low Pressure

Wade R. McGillis*

John S. Fitch

William R. Hamburgren

Van P. Carey**

December, 1990

*Ph.D. candidate at the University of California, Berkeley and a WRL intern.

**Professor of Mechanical Engineering and Applied Science at the University of California, Berkeley.

Abstract

Saturated pool boiling of water at low, sub-atmospheric pressures from a heated, $12.7 \times 12.7 \text{ mm}$ horizontal surface was examined. Rectangular fins, fluidized particulate beds, and surface finishes were used to enhance heat transfer. Water at low pressure significantly decreases the boiling performance below that of water at atmospheric pressure. However, surface temperatures are reduced to values acceptable for cooling electronic components. All rectangular fin geometries were found to enhance heat transfer, although certain geometries were more effective. The finned surfaces extended the base area critical heat flux (CHF) beyond the critical heat flux for the flat plate. Rougher surface finishes reduced wall superheat temperatures. The addition of non-wetting, TFE particles also decreased wall superheat temperatures for the isolated bubble regime. The addition of small copper particles slightly decreased the wall superheat, however, the critical heat flux was significantly reduced. The physical reasons for these trends in the saturated pool boiling enhancements of water at low pressure are discussed.

Portions of this paper will appear at the

*IEEE / CHMT SEMICONDUCTOR THERMAL
AND TEMPERATURE MANAGEMENT
(SEMI-THERM) SYMPOSIUM,*

Phoenix, AZ, February 12-14, 1991.

Copyright © 1990 IEEE

Table of Contents

1. Introduction	1
2. Experimental Apparatus and Procedure	2
3. Results and Discussion	4
3.1. Effect of Pressure	5
3.2. Rectangular Fin Geometries	7
3.3. Effect of Fin Length	8
3.4. Effect of Fin Gap	9
3.5. Effect of Fin Thickness	10
3.6. Grooved Versus Studded Fins	10
3.7. Effect of Surface Finish	11
3.8. Effect of Shallow Fluidized Particulate Beds	12
3.9. CHF for Finned Surfaces	13
4. Conclusions	14
5. References	16
6. Appendix	18

List of Figures

Figure 1:	Test section and system used in low pressure pool boiling experiments.	2
Figure 2:	View of the finned surface and the epoxy which surrounds the copper thermocouple section.	4
Figure 3:	Photograph of boiling water from a finned surface at 4 <i>kPa</i>.	5
Figure 4:	Boiling curves for water at 4, 9, and 101 <i>kPa</i>. CHF was reached in this data. Data of Raben [10] plotted for comparison.	6
Figure 5:	Heat flux versus wall temperature for water at 4, 9, and 101 <i>kPa</i>. CHF was reached in this data.	7
Figure 6:	Effect of fin length for a large fin gap for water at 9 <i>kPa</i>. CHF was not reached in this data.	8
Figure 7:	Effect of fin length for a small fin gap for water at 9 <i>kPa</i>. CHF was not reached in this data.	9
Figure 8:	Effect of fin gap for water at 9 <i>kPa</i>. CHF was not reached in this data.	10
Figure 9:	Effect of fin thickness for water at 9 <i>kPa</i>. CHF was not reached in this data.	11
Figure 10:	Grooved versus Studded Fins. CHF was not reached in this data.	12
Figure 11:	Effect of surface finish for water at 9 <i>kPa</i>. CHF was reached in this data.	13
Figure 12:	The effect of the addition of copper and TFE beads on pool boiling of water at low pressure. CHF was reached in this data.	14
Figure 13:	Critical heat flux characteristics for different fin geometries.	15
Figure 14:	The effects of pressure on a nickel-plated flat plate. Boiling initiated at the interface of the nickel surface and the epoxy due to an adhesion failure. CHF was reached in this data.	18
Figure 15:	The effects of various fin lengths in boiling water at 4 <i>kPa</i>. CHF not reached in this data.	19
Figure 16:	The effects of various beads on a flat plate in water at 4 <i>kPa</i>. CHF was reached in this data.	20
Figure 17:	The effects of beads within a fin array. CHF was not reached in this data.	21
Figure 18:	The effect of various water heights above the flat plate for water at 4 <i>kPa</i>. CHF was reached in all cases. Note the low CHF for the low water level case.	22

1. Introduction

In applications where it is desirable to keep the temperature of a boiling surface low, reducing the saturation pressure may be a useful solution. A reduction in the saturation pressure causes a corresponding decrease in the saturation or boiling temperature. This temperature decrease is translated to the boiling surface. This is particularly useful when water is used as the boiling liquid. Water is a desirable liquid since it has such a high heat of vaporization, high thermal conductivity, and is non-toxic and non-flammable.

Boiling in sealed vessels is a typical application of low pressure boiling. Heat pipes, thermosiphons, and some thermodynamic cycles may rely on low pressures to provide low surface temperatures while moving significant quantities of heat. For example, it is often desirable to maintain a low temperature on the heated end of a heat pipe or thermosiphon in spot cooling electronic components. Heat fluxes from current electronic components are approaching $50 W/cm^2$. These fluxes are not easily handled by solid heat sinks. The use of phase-change heat sinks, which operate with a nearly isothermal interior, is becoming more common. Low temperature operation of these heat sinks may be prescribed by creating a saturated liquid and vapor state in the vessel at very low pressures. Therefore the boiling occurs in the heated end of the vessel at a low temperature.

The characteristics of pool boiling of water at low pressure are much different from pool boiling at atmospheric pressure. An early study reported experimental measurements for a number of liquids boiling at subatmospheric pressures [3]. They discussed the gross effects of low pressure on heat transfer. A much later study investigated saturated nucleate pool boiling of water at subatmospheric pressures from a 38.1 mm diameter horizontal heated surface [10]. Their reported experimental data included the number of bubbles on the surface, frequency of bubble departure and bubble departure diameter for pressures ranging from 1.3 to 101 kPa (101 kPa = 1 atm). The objective of their investigation was to identify the dominant energy transport mechanisms of nucleate boiling and understand how they are affected by pressure. By applying the energy equation to a simple heat transfer model, they presented a theoretical analysis of nucleate boiling. They postulated that free convection, vapor-liquid exchange, and the latent heat of vaporization are the modes in which energy is transferred during saturated nucleate boiling. For very low pressures, they found that the contribution of latent heat was insignificant compared to the vapor-liquid exchange. Measured heat fluxes ranged from about $8 W/cm^2$ at 1.3 kPa to about $19 W/cm^2$ at 101 kPa. Heat fluxes were not extended into the regimes of vapor slugs and columns or critical heat fluxes. Enhancement strategies were not considered either. However, the investigation of Raben et. al. did reveal the vapor bubble formation characteristics for water at low pressure in a large vessel.

The departure of vapor bubbles in water at low pressure has been the subject of several other studies, which have uncovered several important features of this boiling process. Cole and Shulman measured and correlated the effect of pressure on bubble departure diameters from a thin, 12.7×101.6 mm horizontal zirconium ribbon [2]. The data of Raben et. al. and others were included in the comparisons. Others have studied nucleate boiling in an extensive liquid pool of water at subatmospheric pressures [12]. In their experiments, bubble growth rates, frequencies, and departure diameters for different subatmospheric pressures were investigated.

Recently, the boiling regimes of water and acetone at low pressure in a closed two-phase thermosiphon were examined [9]. Experimental and analytical results of the boiling mechanisms were used to examine the regime between intermittent and fully-developed boiling. In their experiments, they measured the bubble departure frequencies as a function of pressure and power. The heated section of their experiment consisted of 200mm long pipes of 12 and 30 mm I.D.

A similar study investigates boiling water at low pressures from a small horizontal thermosiphon surface [5]. Particularly, the surface temperature oscillations caused by the departing, large bubbles are described.

In the present study, some effects of micro and macroscopic surface enhancements for pool boiling water at 4 and 9 kPa are reported. There have been many prior attempts to enhance pool boiling heat transfer by introducing micro and macro surface structures [see for example [4], [7], [8] and [6]]. However, these investigations were performed at atmospheric pressure with either water or halogenated liquids. To the authors' knowledge, no specific information presently exists on surface enhancements for subatmospheric pool boiling of water.

In this investigation, rectangular fin structures of various thicknesses, lengths, and gaps were tested on a horizontal surface. These were compared with baseline cases of flat, horizontal surfaces at various pressures. Since the bubble departure size at low pressures is so large compared to atmospheric boiling, visual observations of the bubble formation and departure were made.

2. Experimental Apparatus and Procedure

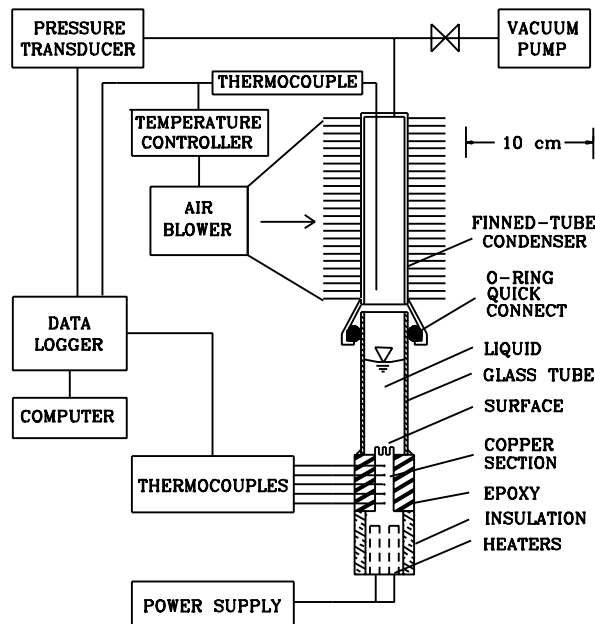


Figure 1: Test section and system used in low pressure pool boiling experiments.

Figure 1 shows the experimental test section and system used in this investigation. The experimental set up allowed many surfaces to be tested in a short period by interchanging

previously prepared test section samples using the quick connect fitting. The copper test sections were machined to accommodate two cartridge heaters in the bottom end. The top half of the copper piece was milled to provide a long $12.7 \times 12.7 \text{ mm}$ square section. Within this section, 0.8 mm holes were drilled to the center to hold thermocouple wires. The copper and thermocouples were then cast in a low viscosity epoxy with good wetting properties.

The size scales that were chosen for this work were comparable to those that might be found in a system used in electronic spot cooling applications. A boiling surface of 1.6 cm^2 was used since it could accommodate a range of typical chip sizes in a thermosiphon application. The main body of the pool boiling container was made with 2.5 cm I.D. tubing. The heat flux ranged from 0 to 100 W/cm^2 in most experiments. In order to examine the CHF, this was extended as high as 230 W/cm^2 . Cool-running electronic components operate more reliably. For this reason, the lowest possible temperature at the boiling surface was desired. The saturation pressure of the experiments was kept at low values of 4 and 9 kPa to obtain saturated temperatures of 29 and 43.6°C respectively.

In order to examine boiling at pressures below 10 kPa for a wide range of surface geometries, certain experimental designs were considered. Nucleate boiling is very dependent on cavity size, distribution, and wetting properties. The most difficult extraneous nucleation sites to control were at the interface where the copper test section was bonded to the epoxy. This interface had to both maintain a vacuum seal and not become a cavity for nucleation. The Ablebond 342-13 epoxy that was eventually selected, adhered and sealed well enough to the copper so that boiling did not occur at the edge where the copper and epoxy met, even after repeated thermal cycling. See Figure 2.

Once the epoxy cured, the top surface of the copper could be machined to the fin geometry of interest. The epoxy was then milled down to be flush with the roots of the fins. This epoxy surface was then bonded to a clear acrylic or glass tube to allow visual observations. To examine another fin geometry, the tube was simply snapped off, a new surface machined, the epoxy cleaned up, and the tube re-attached.

The clear tube fit inside an o-ring fitting at the bottom of the condenser so that repeated assembly was simple. The condenser was made of 125 mm long copper tubing which had radial copper fins wound and soldered onto its O.D. Heat was removed from the fins with an air blower. The top end of the condenser tube was equipped with several sensors. A thermocouple probe extended down through the inside of the tube and could be positioned vertically to monitor fluid temperatures. This thermocouple was used to measure the saturation temperature, T_s , within $\pm 1^\circ \text{C}$.

A transducer measured the internal pressure of the thermosiphon. During initial start up of the system, a valve allowed a high vacuum pump to pull the internal pressure down to very low values. The liquid was boiled during this step to degas the internal volume. Any discrepancy between the measured saturation temperature and that predicted from the measured pressure, indicated the presence of non-condensable gases. Once the system was degassed, the fluid temperature was maintained by a temperature controller. This controller cycled the blower on and off as needed, and proved able to keep the internal pressure constant within $\pm 0.27 \text{ kPa}$.

A datalogger recorded the temperatures of thermocouples embedded in the square copper section and the system pressure. A linear fit of the measured temperature gradient in the copper section was used to calculate the test section heat flux and the temperature at the base of the fins. In this paper, heat flux is defined as the total heat flow through the copper divided by the base area of the test section. Experiments and analyses indicate that the heat losses from the test section were very small, ($< 6\%$), and that the average heat flux at the base of the test surface, q , could be determined within 3%.

Steady state for the entire experiment was determined by monitoring the temperature changes with time via the datalogger and computer. When a particular surface was extended to the critical heat flux (CHF) condition, the final, highest heat flux for which the system reached steady state for nucleate boiling was used as the CHF data point.

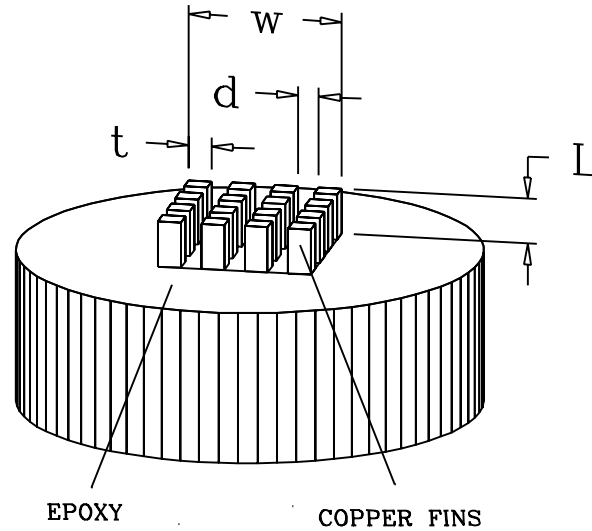


Figure 2: View of the finned surface and the epoxy which surrounds the copper thermocouple section.

The rectangular fin geometry tested is shown in Figure 2. The base of the square heated section, w , was 12.7 mm . Fin gaps, d , were varied from 0.3 to 3.58 mm . Fin lengths, L , were varied from 0 to 10.2 mm . Fin thicknesses, t , were nominally 1.8 mm and 3.6 mm varying only $\pm 0.2 \text{ mm}$. The area in contact with the liquid, or wetted area, is A_w , in cm^2 .

3. Results and Discussion

Nucleate pool boiling heat transfer characteristics and the critical heat flux condition were investigated for a wide range of rectangular fin geometries, for several surface finishes, and with both copper or TFE (e.g. DuPont Teflon) particulate beds. The main objective of this study was to experimentally explore these enhancement techniques on boiling water at subatmospheric pressure. As noted above, water was investigated because of its excellent heat transport properties and because its critical heat flux condition at subatmospheric pressures is significantly greater than that of any fluorocarbon coolants or alcohols. At subatmospheric pressures, water provides the low wall temperatures desired for cooling electronics.

3.1. Effect of Pressure

As a result of the low vapor density at low pressure, the bubbles that form on a surface and their departure diameters are large (large with respect to the container, heated surface, and bubble diameter at higher pressures). These departing bubbles create a large wake which induces mixing and recirculating flow and hence, a removal of superheated liquid from the surface. Consequently, a waiting time is required to reheat the liquid adjacent to the surface to a superheated state. Once this superheated state is reached, a bubble may grow rapidly from any active surface cavity. The waiting time is dependent on the fluid properties, the thermal boundary layer, and the subcooling of the bulk liquid. In short, heat is conducted and convected into the liquid, and bubble departure or ebullition will not take place until enough of the liquid is superheated to support a growing bubble.



Figure 3: Photograph of boiling water from a finned surface at 4 *kPa*.

The internal volume of the thermosiphon used in this investigation was not large (116 cm^3), and liquid occupied 30% of it. The sudden increase in pressure that occurs during the vapor bubble expansion provides an increase in the saturation temperature. The increase of the saturation temperature causes an instantaneous subcooling of the liquid, which gets mixed in the wake of large departing bubbles.

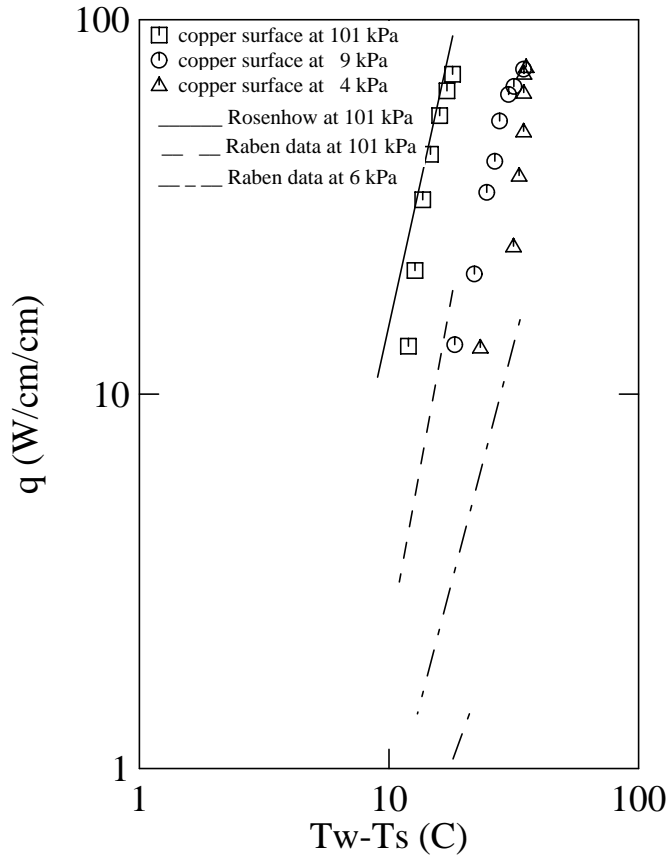


Figure 4: Boiling curves for water at 4, 9, and 101 *kPa*. CHF was reached in this data. Data of Raben [10] plotted for comparison.

At low pressure, much larger superheats are generally required, fewer active sites are available and thus, the waiting time can become quite long. During the waiting time, the wall temperature increases until a bubble departs. The surface is then cooled by liquid reflooding from the far field. Heat flux versus temperature data that are reported in this paper are averaged; fluctuation of the heated surface temperature is not reported.

A reduction in the pressure for a saturated water system leads to higher wall superheat or excess temperature (wall temperature minus saturated fluid temperature or $T_w - T_s$) as shown in Figure 4. However, the decrease in the saturation temperature at lower pressures provides the benefit of lower wall temperatures as shown in Figure 5. The poorer performance of the heat transfer mechanisms at low pressure (the shift in the boiling curves to higher excess surface temperatures for a given heat flux as shown in Figure 4) may be attributed to a combination of effects. Lower pressures result in lower vapor densities and larger bubbles. The lower pressure increases the critical site radius on a surface. This tends to decrease the number of active bubble nucleation sites and increases the wall superheat which allows bubbles to depart from the surface.

Lines fitted to the data of Raben et. al. [10] for atmospheric and subatmospheric pressure are plotted in Figure 4. The heat flux data of Raben et. al. is lower than the data of this study for both pressures compared. Part of this discrepancy might be accounted for by the fact that the test

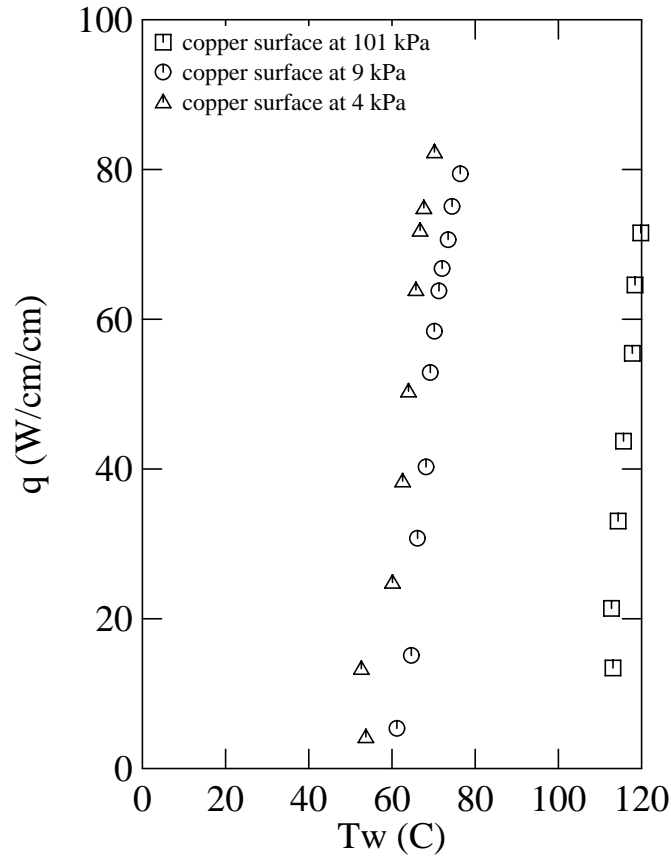


Figure 5: Heat flux versus wall temperature for water at 4, 9, and 101 *kPa*. CHF was reached in this data.

sections weren't identical. In their experiment, the boiling surface was extensively polished. This may have reduced the number of surface cavities of critical size and therefore increased the wall superheat required to support the level of nucleation needed to deliver the specified heat flux.

A line corresponding to the Rosenhow correlation of nucleate boiling data for water on a copper surface is also plotted in Figure 4 [11]. Rosenhow correlated boiling data for pressures ranging from 101 to 16,936 *kPa*. There seems to be a fairly good agreement between this correlation, with properties evaluated at the proper pressures, and the data of this investigation.

3.2. Rectangular Fin Geometries

One of the major interests of the present study was to determine the effect of fin geometry on nucleate boiling of water at low pressure from a heated horizontal section. A number of rectangular fin arrays were machined into boiling surfaces to augment convective and nucleate boiling heat transfer. The effects of different fin geometries were determined by parametric experiments and are discussed below.

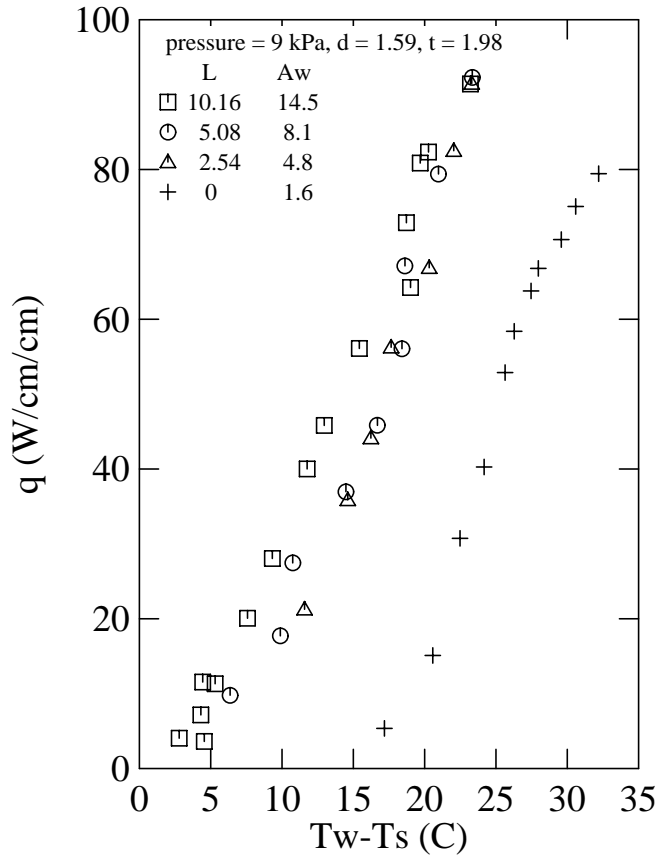


Figure 6: Effect of fin length for a large fin gap for water at 9 kPa. CHF was not reached in this data.

3.3. Effect of Fin Length

Data for finned surfaces with varying fin length are plotted in Figures 6 and 7. All the finned surfaces significantly extended the nucleate boiling range beyond that obtained for a flat plate ($L=0$). Figures 6 and 7 also show that for two different fin gaps and a nominal fin thickness of 1.8 mm, there seems to be no significant heat transfer enhancement for fin lengths greater than 2.54 mm. This implies that for a given fin thickness, there exists a certain fin length beyond which the increase in fin effectiveness is small.

Note that for the boiling with fins, there will always be a heat transfer enhancement due to the added cavity site at the intersection of the fin and the base. This site could not be controlled easily and is probably large in size. Since boiling at low pressure only relies on one or two large, active cavities, all finned surfaces should enhance heat transfer beyond that of a very rough surface.

In our experiments with the finned surfaces, the transition to film boiling occurred at very high heat fluxes. The corresponding high wall temperatures and the expansion coefficient mismatch between the epoxy and the copper, would cause a seal failure. For this reason, only limited CHF data was obtained for finned geometries.

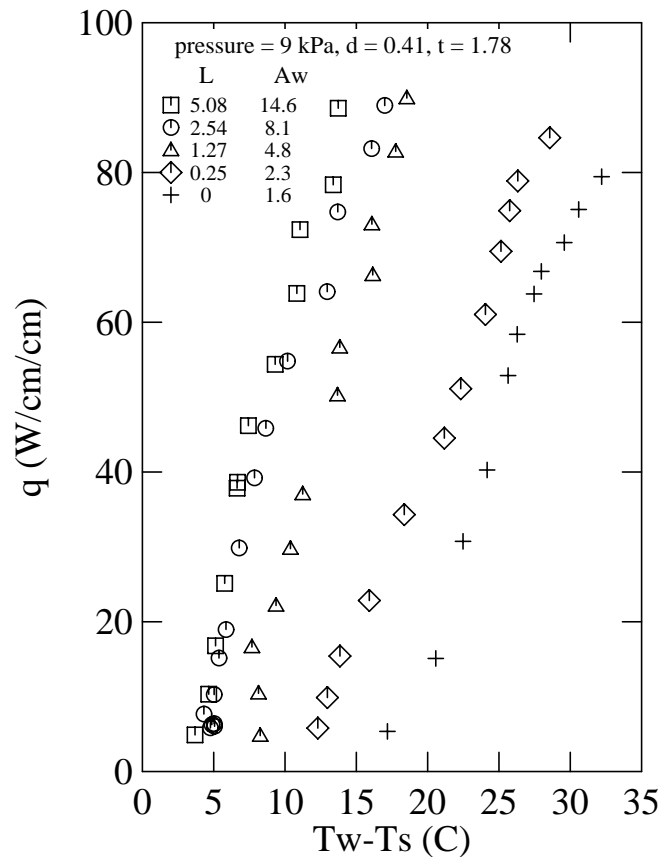


Figure 7: Effect of fin length for a small fin gap for water at 9 kPa. CHF was not reached in this data.

3.4. Effect of Fin Gap

Fin gaps were found to have a strong effect on the heat transfer performance. Boiling curves for different fin geometries with varying fin gaps are plotted in Figure 8. For a fin height of 2.54 mm and a nominal fin thickness of about 1.8 mm, the fin gaps ranged from 0.3 to 3.58 mm. Smaller fin gaps exhibit significantly higher heat fluxes for a given wall superheat. Compared to the flat plate dissipating 60 W/cm^2 , the largest fin gap, $d=3.58 \text{ mm}$, provides a 28% decrease in the wall superheat, and the smallest fin gap, $d=0.3 \text{ mm}$, decreased the superheat by 72%. This may be due, in part, to the increased wetted area. However, the increased surface area does not account for all of the increase in performance. For example, the fin with $d=0.3 \text{ mm}$ is a much better performer than the fin with $d=0.41 \text{ mm}$ even though the wetted areas are almost identical. For this reason, another mechanism is believed to be present.

The boiling characteristics at low pressure are such that the surface is not uniformly covered with active nucleation sites. In fact, only one or two sites were observed to be actually active throughout the isolated bubble boiling regime. Most of the enhanced surfaces, therefore, are only in contact with circulating liquid. At smaller fin gaps, restricted flow exists between fins. The circulating flow resulting from ebullition may be unable to effectively replenish all the fluid between the tightly-grouped fins. As a result, heated fluid does not get carried away quickly and

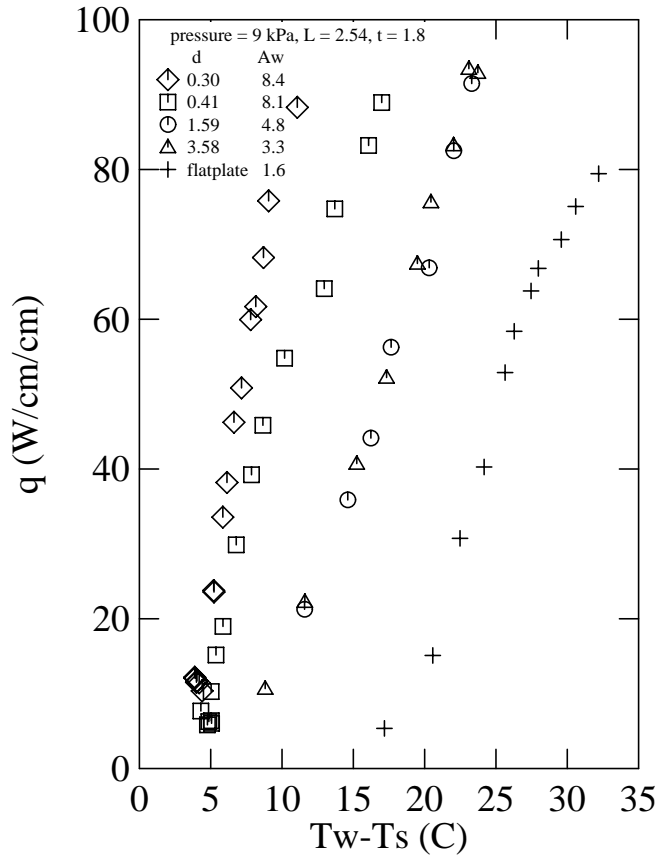


Figure 8: Effect of fin gap for water at 9 kPa. CHF was not reached in this data.

the waiting time required to heat the small volume of liquid between the fins to temperatures suitable for bubble formation is reduced [9]. This may increase the frequency of bubble departure. In contrast, for the larger gaps between fins, it appears that the heated fluid between fins can easily be carried away by the circulating flow and the waiting time increases.

3.5. Effect of Fin Thickness

Figure 9 is a plot of two fin geometries having the same fin gap and fin height. There seems to be no significant difference in the performance of different fin thicknesses even though the wetted area is different. Since each of the many fins is made of copper and carries only a small portion of the total heat load, the fin effectiveness may be adequately high in the dimensions examined.

3.6. Grooved Versus Studded Fins

Although our study was primarily concerned with the effect of rectangular studded fins, data was taken for grooved fins, those which have a gap, d , in only one direction. Figure 10 compares boiling curves between grooved and studded fin geometries. Notice that the fins compared in Figure 10 have the same wetted area. The slight increase in performance of the studded fins may be attributed to differing liquid replenishment or the increase in cavity sites at the base of the fins.

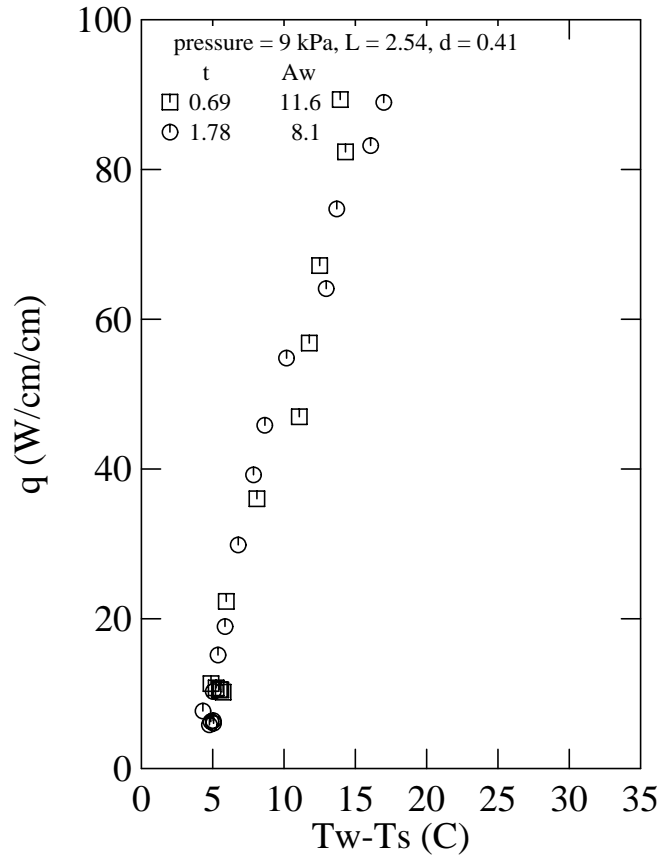


Figure 9: Effect of fin thickness for water at 9 kPa. CHF was not reached in this data.

3.7. Effect of Surface Finish

The effects of surface finish on nucleate pool boiling of water at subatmospheric pressure were investigated by comparing boiling curves for copper surfaces with different surface roughnesses. Figure 11 shows that a rougher surface increased the heat transfer performance. For a wall superheat of 25° C, an increase in surface roughness from 0.16 to 5.72 $\mu\text{m rms}$ provides about a 100% increase in heat flux. This increase is typical for nucleate boiling, since a rougher surface may provide a larger population of critically-sized surface cavities. A larger active cavity generally results in bubble departure at lower wall superheat temperatures.

Large surface features do not necessarily mean larger active cavities. Bubble nucleation also depends on nucleate embryos (absorbed gases and vapors), vapor density, heat of vaporization, and surface tension. Large cavities have a greater risk of losing their vapor embryos, and consequently may not become active. Since low pressure boiling relies on a small number of large cavities, the boiling heat transfer enhancement with rough surfaces may not be as great as the enhancement at high pressures where there is a significant increase in the number of active sites.

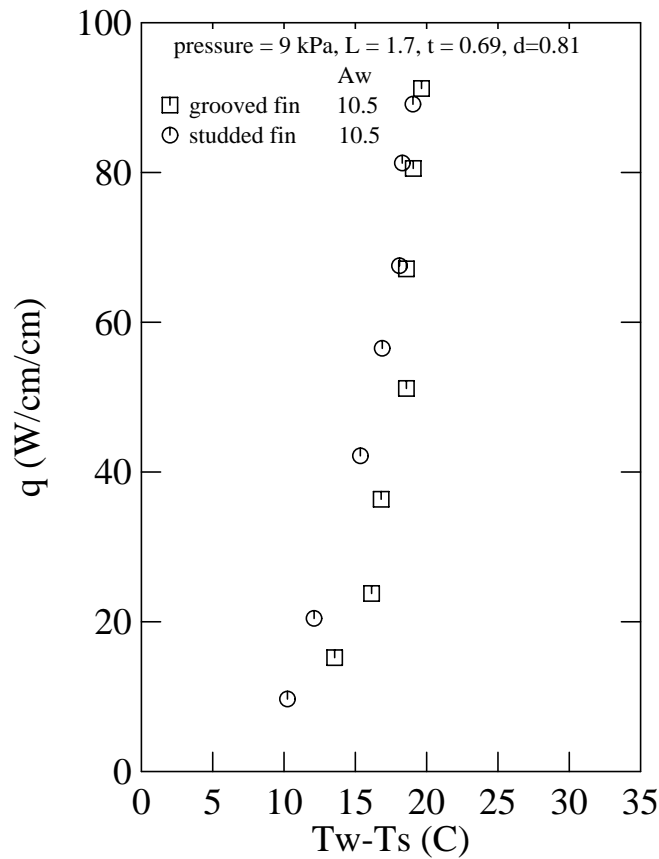


Figure 10: Grooved versus Studded Fins. CHF was not reached in this data.

3.8. Effect of Shallow Fluidized Particulate Beds

Experimental data presented in Figure 12 show the effects of nucleate boiling enhancement using unconfined copper or TFE particles. While previously reported data indicate the effects of thin layers of copper or glass beads in a saturated pool boiling system using water at 1 atm [1], the data of this investigation was taken at much lower pressures. The objective of the experiments reported here was to determine if unconfined particles would enhance boiling heat transfer from a small horizontal heated surface. Using the same test system and section described above, copper or TFE beads were added to the flat surface.

The enhancement due to bead nucleation sites should be most noticeable for smooth surfaces and at low superheats. Rough surfaces already have active nucleation sites and the presence of particles should not contribute to bubble nucleation. It was found that the copper beads did not significantly enhance the nucleation behavior. This is probably because no large critical cavity sites are introduced by adding small copper beads. However, because TFE is non-wetting, active cavities on the TFE beads are plentiful and act as seeds for nucleation. The TFE bead cavities adjacent to the superheated copper surface can easily become active, thus reducing the wall superheat temperature of the surface.

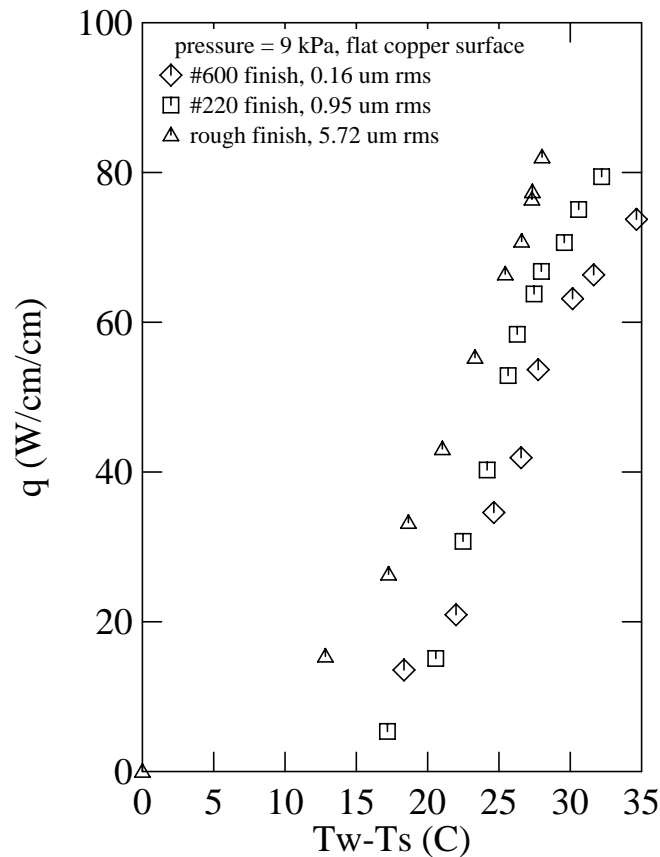


Figure 11: Effect of surface finish for water at 9 kPa. CHF was reached in this data.

At higher heat fluxes, the heavy copper beads remained on the bottom and hindered the return of liquid to the heated surface, leading to a lower CHF. The TFE beads, being more buoyant, were mixed throughout the moving liquid and did not decrease the CHF.

3.9. CHF for Finned Surfaces

In addition to the enhanced nucleate boiling that fins provide, the critical heat flux for finned surfaces was found to be significantly increased over that of the flat surface, as shown in Figure 13. In fact, for the fin geometry with the smallest fin gap ($d=0.3$, $t=1.8$, $L=2.54$), there was a 150% increase in the critical heat flux over the flat plate. While geometries with larger fin gaps perform similarly to a flat plate in the nucleate boiling range, their critical heat fluxes are different.

Critical heat flux for wide fin gap geometries is approached very gradually, as seen in Figure 13. This may be due to the fact that the vapor film which is required for film boiling is not stable for wide fin gaps. Part of the surface may be in film boiling while other parts are wetted by liquid. Photographic observations show that the vapor film at critical heat flux for these wide gaps has a wavy appearance and is thick in the region near the base of the fins. In contrast, for the flat plate and small fin gap geometries, the transition to film boiling is abrupt.

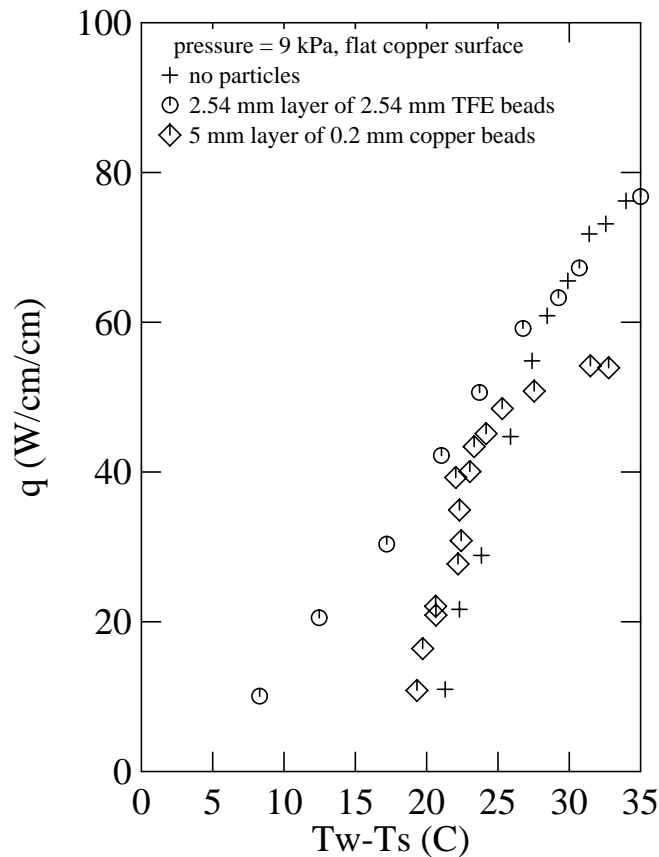


Figure 12: The effect of the addition of copper and TFE beads on pool boiling of water at low pressure. CHF was reached in this data.

Water has such a high heat of vaporization that only a small amount of liquid volume is required to vaporize in order to remove a significant amount of heat. For this reason, even at the small fin gaps, the volume of liquid contained between the fins is enough to support a great deal of latent heating and subsequent convective cooling. Since only small amounts of liquid are removed from the fins during vaporization, replenishment of that liquid is easily possible, avoiding a significant premature dryout between the close-packed fins used in these experiments.

4. Conclusions

Pool boiling enhancement techniques on a horizontal surface in a thermosiphon were explored for water at subatmospheric pressures. Rectangular finned geometries, particulate beds of copper or TFE beads, and different surface finishes were investigated. Our results support the following conclusions:

1. With various enhancements, the regimes of low pressure boiling water were similar to those previously observed in round tubes, from thin heated wires, or from extensive horizontal surfaces. At low heat flux levels only one or two nucleation sites are active, the frequency of bubble departure is low and the departure diameter is large. The bubble departure frequency increases with heat flux.

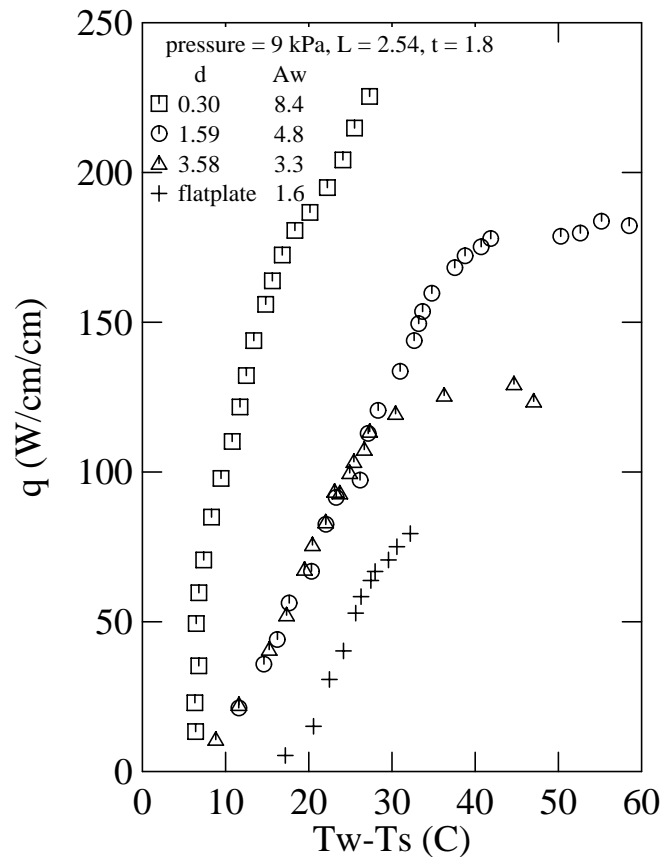


Figure 13: Critical heat flux characteristics for different fin geometries.

2. Low bubble departure frequencies (long waiting times) lead to wall temperature oscillations. For low pressure pool boiling water, heat fluxes greater than 60 W/cm^2 were required to produce a departure frequency high enough to maintain a steady wall temperature.

3. The size and geometry of surface enhancements affect the bubble formation, release mechanisms, and convective heat transport. Surface enhancements often decrease the wall superheat and waiting time significantly.

4. For finned geometries, there is a certain fin height beyond which the performance is not significantly increased. For example, the height is about 2.54 mm for a fin thickness of about 1.8 mm .

5. The liquid within small fin gaps heats up more quickly than liquid between large fin gaps. Small fin gaps also increase the wetted area available for heat transfer. These combine to make the small fin gaps more effective at initiating boiling and shortening the waiting time. This reduces the magnitude of the temperature oscillations in the heated wall.

6. In the geometries examined, copper fin thickness was not influential.

7. Adding fins to a flat surface can increase the CHF (based on the nominal heated area) by more than 150%.

8. Copper beads of 0.2 mm diameter did not improve boiling at low heat fluxes, and decreased the CHF.
9. Non-wetting TFE beads lowered the wall superheat at low heat fluxes by providing nucleation sites, but they did not change the performance at high heat fluxes. TFE beads, or other non-wetting particles, may be useful in reducing the waiting time and therefore the temperature oscillations in the heated wall.
10. Rougher surfaces may provide larger cavities that are required for low pressure boiling, thereby reducing the wall superheat. However, the gas embryo that exists in a large cavity can also be easily washed away, leading to a large waiting time before boiling recurs.

5. References

- [1] Y. K. Chuah and V. P. Carey.
Boiling Heat Transfer in a Shallow Fluidized Particulate Bed.
Journal of Heat Transfer 109:196-203, February, 1987.
- [2] R. Cole and H. L. Shulman.
Bubble Departure Diameters at Subatmospheric Pressures.
Chemical Engineering Progresses Symposium Series 62(64):6-16, 1967.
- [3] D. S. Cryder and A. C. Finalborgo.
Heat Transmission from Metal Surfaces to Boiling Liquids; Effect of Temperature of the Liquid on the Liquid Film Coefficient.
American Institute of Chemical Engineers 33:346-362, 1937.
- [4] K. W. Haley and J. W. Westwater.
Boiling Heat Transfer from Single Fins.
In *Proceedings of the ASME/AIChE National Heat Transfer Conference*, pages 245-253.
ASME/AIChE National Heat Transfer Conference, 1966.
- [5] W. R. McGillis, V. P. Carey, J. S. Fitch, and W. R. Hamburgren.
Pool Boiling on a Small Heat Dissipating Element in Water at Low Pressure.
July, 1991.
To be presented at the 1991 ASME/AIChE National Heat Transfer Conference, Minneapolis Minnesota.
- [6] I. Mudawar and T. M. Anderson.
High Flux Electronic Cooling by Means of Pool Boiling - Part II. Optimization of Enhanced Surface Geometry.
In *Proceedings of the National Heat Transfer Conference*, pages 35-49. 1989 National Heat Transfer Conference, Philadelphia, Pennsylvania, August, 1989.
- [7] W. Nakayama, T. Daikoku, H. Kuwahara, and T. Nakajima.
Dynamic Model of Enhanced Boiling Heat Transfer on Porous Surfaces, Part I: Experimental Investigation.
Journal of Heat Transfer 102:445-450, August, 1980.

- [8] W. Nakayama, T. Nakajima, and S. Hirasawa.
Heat Sink Studs Having Enhanced Boiling Surfaces for Cooling of Microelectronic Components.
In *Proceedings of the ASME Winter Annual Meeting*. ASME Paper 84-WA/HT-89, 1984.
- [9] A. Niro and G. P. Beretta.
Boiling Regimes in a Closed Two-Phase Thermosyphon.
International Journal of Heat and Mass Transfer 33(10):2099-2110, 1990.
- [10] I. A. Raben, R. T. Beaubouef, and G. E. Commerford.
A Study of Heat Transfer in Nucleate Pool Boiling of Water at Low Pressure.
Chemical Engineering Progresses Symposium Series 61(57):249-257, 1965.
- [11] W. M. Rosenhow.
Handbook of Heat Transfer.
McGraw-Hill, New York, 1952.
W. M. Rosenhow and J. P. Hartnett ed., Section 13.
- [12] S. J. D. Van Stralen, R. Cole, W.M. Sluyter, and M. S. Sohal.
Bubble Growth Rates in Nucleate Boiling of Water at Subatmospheric Pressures.
International Journal of Heat and Mass Transfer 18:655-669, 1975.

6. Appendix

The figures below present data from additional tests that were run during this work.

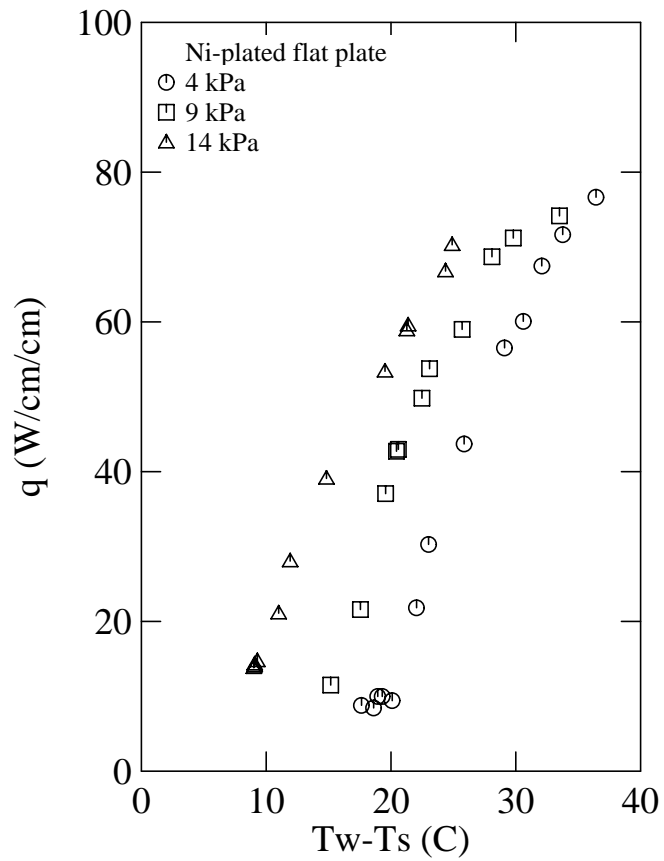


Figure 14: The effects of pressure on a nickel-plated flat plate. Boiling initiated at the interface of the nickel surface and the epoxy due to an adhesion failure. CHF was reached in this data.

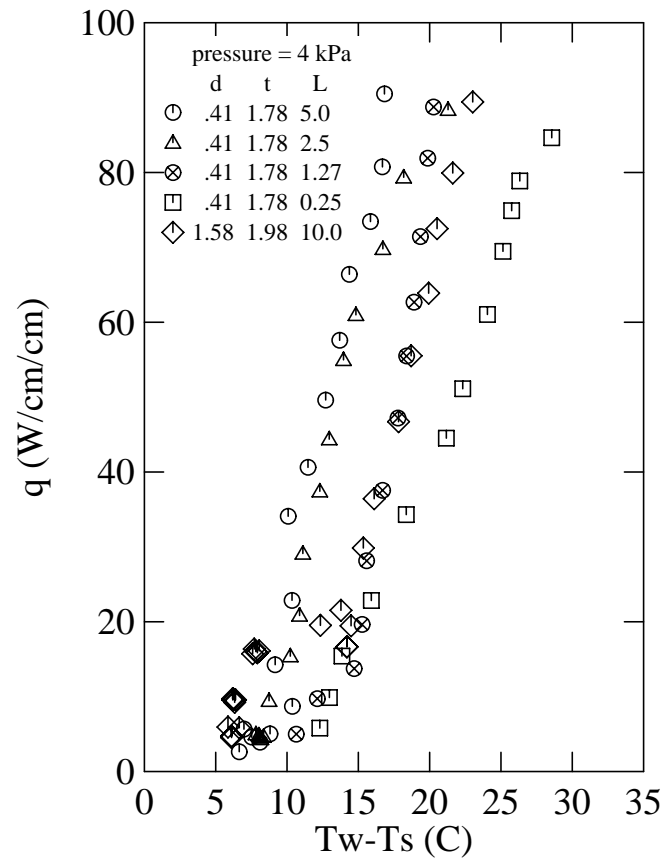


Figure 15: The effects of various fin lengths in boiling water at 4 kPa. CHF not reached in this data.

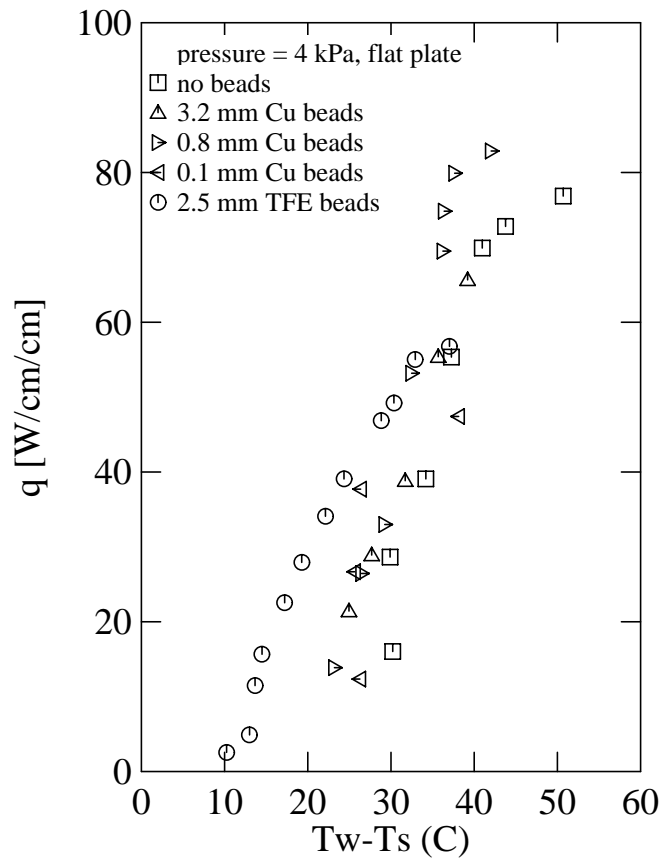


Figure 16: The effects of various beads on a flat plate in water at 4 *kPa*. CHF was reached in this data.

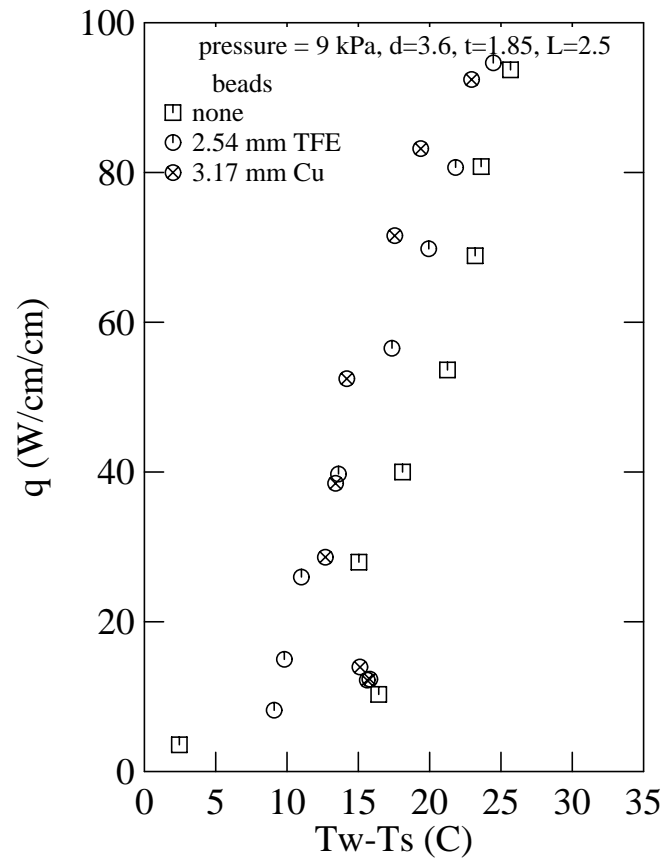


Figure 17: The effects of beads within a fin array. CHF was not reached in this data.

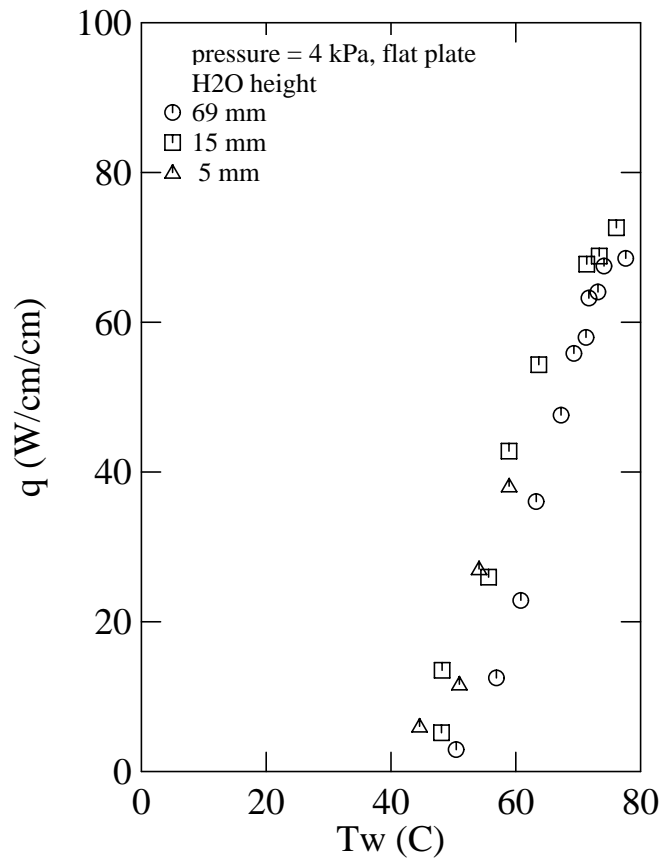


Figure 18: The effect of various water heights above the flat plate for water at 4 kPa. CHF was reached in all cases. Note the low CHF for the low water level case.

WRL Research Reports

“Titan System Manual.”

Michael J. K. Nielsen.

WRL Research Report 86/1, September 1986.

“Global Register Allocation at Link Time.”

David W. Wall.

WRL Research Report 86/3, October 1986.

“Optimal Finned Heat Sinks.”

William R. Hamburgren.

WRL Research Report 86/4, October 1986.

“The Mahler Experience: Using an Intermediate Language as the Machine Description.”

David W. Wall and Michael L. Powell.

WRL Research Report 87/1, August 1987.

“The Packet Filter: An Efficient Mechanism for User-level Network Code.”

Jeffrey C. Mogul, Richard F. Rashid, Michael J. Accetta.

WRL Research Report 87/2, November 1987.

“Fragmentation Considered Harmful.”

Christopher A. Kent, Jeffrey C. Mogul.

WRL Research Report 87/3, December 1987.

“Cache Coherence in Distributed Systems.”

Christopher A. Kent.

WRL Research Report 87/4, December 1987.

“Register Windows vs. Register Allocation.”

David W. Wall.

WRL Research Report 87/5, December 1987.

“Editing Graphical Objects Using Procedural Representations.”

Paul J. Asente.

WRL Research Report 87/6, November 1987.

“The USENET Cookbook: an Experiment in Electronic Publication.”

Brian K. Reid.

WRL Research Report 87/7, December 1987.

“MultiTitan: Four Architecture Papers.”

Norman P. Jouppi, Jeremy Dion, David Boggs, Michael J. K. Nielsen.

WRL Research Report 87/8, April 1988.

“Fast Printed Circuit Board Routing.”

Jeremy Dion.

WRL Research Report 88/1, March 1988.

“Compacting Garbage Collection with Ambiguous Roots.”

Joel F. Bartlett.

WRL Research Report 88/2, February 1988.

“The Experimental Literature of The Internet: An Annotated Bibliography.”

Jeffrey C. Mogul.

WRL Research Report 88/3, August 1988.

“Measured Capacity of an Ethernet: Myths and Reality.”

David R. Boggs, Jeffrey C. Mogul, Christopher A. Kent.

WRL Research Report 88/4, September 1988.

“Visa Protocols for Controlling Inter-Organizational Datagram Flow: Extended Description.”

Deborah Estrin, Jeffrey C. Mogul, Gene Tsudik, Kamaljit Anand.

WRL Research Report 88/5, December 1988.

“SCHEME->C A Portable Scheme-to-C Compiler.”

Joel F. Bartlett.

WRL Research Report 89/1, January 1989.

“Optimal Group Distribution in Carry-Skip Adders.”

Silvio Turrini.

WRL Research Report 89/2, February 1989.

“Precise Robotic Paste Dot Dispensing.”

William R. Hamburgren.

WRL Research Report 89/3, February 1989.

- “Simple and Flexible Datagram Access Controls for Unix-based Gateways.”
 Jeffrey C. Mogul.
 WRL Research Report 89/4, March 1989.
- “Spritely NFS: Implementation and Performance of Cache-Consistency Protocols.”
 V. Srinivasan and Jeffrey C. Mogul.
 WRL Research Report 89/5, May 1989.
- “Available Instruction-Level Parallelism for Superscalar and Superpipelined Machines.”
 Norman P. Jouppi and David W. Wall.
 WRL Research Report 89/7, July 1989.
- “A Unified Vector/Scalar Floating-Point Architecture.”
 Norman P. Jouppi, Jonathan Bertoni, and David W. Wall.
 WRL Research Report 89/8, July 1989.
- “Architectural and Organizational Tradeoffs in the Design of the MultiTitan CPU.”
 Norman P. Jouppi.
 WRL Research Report 89/9, July 1989.
- “Integration and Packaging Plateaus of Processor Performance.”
 Norman P. Jouppi.
 WRL Research Report 89/10, July 1989.
- “A 20-MIPS Sustained 32-bit CMOS Microprocessor with High Ratio of Sustained to Peak Performance.”
 Norman P. Jouppi and Jeffrey Y. F. Tang.
 WRL Research Report 89/11, July 1989.
- “The Distribution of Instruction-Level and Machine Parallelism and Its Effect on Performance.”
 Norman P. Jouppi.
 WRL Research Report 89/13, July 1989.
- “Long Address Traces from RISC Machines: Generation and Analysis.”
 Anita Borg, R.E.Kessler, Georgia Lazana, and David W. Wall.
 WRL Research Report 89/14, September 1989.
- “Link-Time Code Modification.”
 David W. Wall.
 WRL Research Report 89/17, September 1989.
- “Noise Issues in the ECL Circuit Family.”
 Jeffrey Y.F. Tang and J. Leon Yang.
 WRL Research Report 90/1, January 1990.
- “Efficient Generation of Test Patterns Using Boolean Satisfiability.”
 Tracy Larrabee.
 WRL Research Report 90/2, February 1990.
- “Two Papers on Test Pattern Generation.”
 Tracy Larrabee.
 WRL Research Report 90/3, March 1990.
- “Virtual Memory vs. The File System.”
 Michael N. Nelson.
 WRL Research Report 90/4, March 1990.
- “Efficient Use of Workstations for Passive Monitoring of Local Area Networks.”
 Jeffrey C. Mogul.
 WRL Research Report 90/5, July 1990.
- “A One-Dimensional Thermal Model for the VAX 9000 Multi Chip Units.”
 John S. Fitch.
 WRL Research Report 90/6, July 1990.
- “1990 DECWRL/Livermore Magic Release.”
 Robert N. Mayo, Michael H. Arnold, Walter S. Scott, Don Stark, Gordon T. Hamachi.
 WRL Research Report 90/7, September 1990.
- “Pool Boiling Enhancement Techniques for Water at Low Pressure.”
 Wade R. McGillis, John S. Fitch, William R. Hambrgen, Van P. Carey.
 WRL Research Report 90/9, December 1990.

WRL Technical Notes

“TCP/IP PrintServer: Print Server Protocol.”

Brian K. Reid and Christopher A. Kent.

WRL Technical Note TN-4, September 1988.

“TCP/IP PrintServer: Server Architecture and Implementation.”

Christopher A. Kent.

WRL Technical Note TN-7, November 1988.

“Smart Code, Stupid Memory: A Fast X Server for a Dumb Color Frame Buffer.”

Joel McCormack.

WRL Technical Note TN-9, September 1989.

“Why Aren’t Operating Systems Getting Faster As Fast As Hardware?”

John Ousterhout.

WRL Technical Note TN-11, October 1989.

“Mostly-Copying Garbage Collection Picks Up Generations and C++.”

Joel F. Bartlett.

WRL Technical Note TN-12, October 1989.

“Limits of Instruction-Level Parallelism.”

David W. Wall.

WRL Technical Note TN-15, December 1990.

“The Effect of Context Switches on Cache Performance.”

Jeffrey C. Mogul and Anita Borg.

WRL Technical Note TN-16, December 1990.

“MTOOL: A Method For Detecting Memory Bottlenecks.”

Aaron Goldberg and John Hennessy.

WRL Technical Note TN-17, December 1990.

“Predicting Program Behavior Using Real or Estimated Profiles.”

David W. Wall.

WRL Technical Note TN-18, December 1990.